Acylation state of the phosphatidylinositol hexamannosides from Mycobacterium bovis bacillus Calmette Guerin and mycobacterium tuberculosis H37Rv and its implication in Toll-like receptor response.

Martine Gilleron, Valérie Quesniaux, Germain Puzo

THE JOURNAL OF BIOLOGICAL CHEMISTRY
Vol. 278, No. 32, Issue of August 8, pp. 29880–29889, 2003
Printed in U.S.A.

Acylation State of the Phosphatidylinositol Hexamannosides from *Mycobacterium bovis* Bacillus Calmette Guérin and *Mycobacterium tuberculosis* H37Rv and Its Implication in Toll-like Receptor Response*

Received for publication, April 3, 2003, and in revised form, May 20, 2003
Published, JBC Papers in Press, May 29, 2003, DOI 10.1074/jbc.M303446200

Martine Gilleron‡§, Valérie F. J. Quesniaux¶, and Germain Puzo‡

From the ‡Institut de Pharmacologie et de Biologie Structurale du CNRS, 205 Route de Narbonne, 31077 Toulouse Cedex and ¶FRE 2358, Experimental and Molecular Genetics, 3B rue de la Ferrolerie, 45071 Orleans, Cedex 2, France

The dimannoside (PIM_2) and hexamannoside (PIM_6) phosphatidyl-*myo*-inositol mannosides are the two most abundant classes of PIM found in *Mycobacterium bovis* bacillus Calmette Guérin, *Mycobacterium tuberculosis* H37Rv, and *Mycobacterium smegmatis* 607. Recently, these long known molecules received a renewed interest due to the fact that PIM_2 constitute the anchor motif of an important constituent of the mycobacterial cell wall, the lipoarabinomannans (LAM), and that both LAM (phosphoinositol-capped LAM) and PIM are agonists of Toll-like receptor 2 (TLR2), a pattern recognition receptor involved in innate immunity. Due to the biological importance of these molecules, the chemical structure of PIM was revisited. The structure of PIM_2 was recently published (Gilleron, M., Ronet, C., Mempel, M., Monsarrat, B., Gachelin, G., and Puzo, G. (2001) *J. Biol. Chem.* 276, 34896–34904). Here we report the purification and molecular characterization of PIM_6 in their native form. For the first time, four acyl forms of this molecule have been purified, using hydrophobic interaction chromatography. Mono- to tetra-acylated molecules were identified in *M. bovis* bacillus Calmette Guérin, *M. tuberculosis* H37Rv, and *M. smegmatis* 607 using a sophisticated combination of analytical tools, including matrix-assisted laser desorption/ionization-time of flight-mass spectrometry and two-dimensional homo- and heteronuclear NMR spectroscopy. These experiments revealed that the major acyl forms are similar to the ones described for PIM_2. Finally, we show that PIM_6, like PIM_2, activate primary macrophages to secrete TNF-α through TLR2, irrespective of their acylation pattern, and that they signal through the adaptor MyD88.

A variety of phosphatidyl-*myo*-inositol mannosides (PIM)[1]-based compounds are known to be part of the mycobacterial cell wall. Among these compounds are the lipoarabinomannans (LAM) and the lipomannans (LM). The importance of these lipoglycans in the immunopathogenesis of tuberculosis is now established, and a rising number of studies in the literature are devoted to the delineation of their biological activities (2, 3). PIM, LM, and LAM derive from the same biosynthetic pathway as demonstrated using biochemical (1, 2, 4, 5) and genetic approaches (6–8). PIM appear to be the common anchor of LM and LAM, as LM correspond to polymannosylated PIM and then give rise to LAM by further glycosylation with arabinosyl units. This anchor plays a fundamental role in the biological functions of LAM. Indeed, it is now clearly established that most of the LAM immunoregulatory effects are abolished by alkaline hydrolysis, highlighting the importance of the lipidic part of the anchor (2).

Mycobacterium bovis BCG 1173P2 (the Pasteur strain) (1), *Mycobacterium smegmatis* ATCC-607 (1), and *Mycobacterium tuberculosis* H37Rv ATCC-27294 were found to mainly contain two PIM families, the dimmanosylated (PIM_2) and the hexamannosylated (PIM_6) ones. PIM_1, PIM_3, PIM_4, and PIM_5 were observed in very small amounts, suggesting that they are biosynthetic intermediates.

PIM are known from the 1940s and have been structurally investigated by Ballou and co-workers in the 1960s (9). By 1965, studies of deacylated PIM from *M. tuberculosis* and *Mycobacterium phlei* revealed the structure of the saccharidic part. PIM_6 were the highest PIM which were fully characterized from *M. phlei* (10) and were shown to contain a pentamannoside of sequence Man*p*α1→2Man*p*α1→2Man*p*α1→6Man*p*α1→6Man*p*α1→ attached to position 6 of the *myo*-inositol, whereas a Man*p* unit is linked to the position 2 of the *myo*-inositol. Recently, the complete structure of native PIM_2 has been achieved (1, 2). These last studies focused on the characterization of their lipidic part and unambiguously established the existence of a tetra-acylated form that was thus far suggested (4).

Several biological functions have been recently attributed to PIM. PIM_2 were shown to recruit natural killer T cells, which have a primary role in the local granulomatous response (1, 11). Moreover, a role for surface-exposed PIM as *M. tuberculosis* adhesins that mediate attachment to non-phagocytic cells has also been established (12, 13). Analysis of infected macrophages revealed that PIM, among other mycobacterial lipids, are actively trafficked out of the mycobacterial phagosome (14). This could be of particular importance relating to the potential

* This work was supported by the European Community through the Fifth Framework Program TB vaccine program. The costs of publication of this article were defrayed in part by the payment of page charges. This article must therefore be hereby marked "*advertisement*" in accordance with 18 U.S.C. Section 1734 solely to indicate this fact.

§ To whom correspondence should be addressed. Tel.: 33 5 61 17 55 57; Fax: 33 5 61 17 59 94, E-mail: Martine.Gilleron@ipbs.fr.

[1] The abbreviations used are: PIM, phosphatidyl-*myo*-inositol mannosides; BCG, bacillus Calmette Guérin; BLP, bacterial lipopeptide; C_{16}, palmitate; C_{18}, stearate; C_{19}, tuberculostearate (10-methyloctadecanoate); COSY, correlation spectroscopy; ESI-MS, electrospray ionization-mass spectrometry; Gro, glycerol; HABA, 2-(4-hydroxyphenylazo)-benzoic acid; HMQC, heteronuclear multiple quantum correlation spectroscopy; HOHAHA, homonuclear Hartmann-Hahn spectroscopy; LAM, lipoarabinomannans; LM, lipomannans; ManLAM, LAM with mannosyl extensions; MALDI-*Tof*-MS, matrix-assisted laser desorption/ionization-time of flight-mass spectrometry; *myo*-Ins, *myo*-inositol; MyD88, myeloid differentiation factor; *p*, pyranosyl; PI, phosphatidyl-*myo*-inositol; QMA, quaternary methyl ammonium; ROESY, rotating frame nuclear Overhauser effect spectroscopy; t, terminal; TLR, Toll-like receptor; TMS, trimethylsilyl; TNF-α, tumor necrosis factor-α; IL, interleukin; LPS, lipopolysaccharide.

role played by these constituents in extending the influence of the bacterium over its surroundings. An unfractionated preparation of PIM, as well as phosphoinositol capped LAM (PI-LAM), was recently shown to activate cells via Toll-like receptor-2 (TLR-2) (15). Activation of TLR-dependent signaling pathways leads to the activation of genes that participate in innate immune responses, such as expression of cytokines, coactivation molecules, and nitric oxide (16, 17). Finally, PIM_6 as well as ManLAM from *Mycobacterium leprae* and *M. tuberculosis* are presented by antigen-presenting cells in the context of CD1b (18). The high affinity interaction of CD1b molecules with the PIM_2 acyl side chains was then established (19). The phosphatidylinositol moiety plays a central role in the process of PIM and ManLAM binding to CD1b proteins.

Here we investigated the structure of the most polar PIM isolated from *M. bovis* BCG, PIM_6. The earlier NMR studies conducted on PIM_2 and PIM_6 by Severn *et al.* (20) focused on the deacylated molecules, thus excluding the study of the lipidic moieties. In this study, we investigated the chemical structure of native PIM_6, focusing on the characterization of the different "acyl forms," using sophisticated analytical tools such as MALDI-MS and two-dimensional NMR. Then we demonstrated the capacity of the PIM_2 and PIM_6 acyl forms to stimulate macrophages to produce cytokines, and we investigated the implication of the different TLR in this process.

EXPERIMENTAL PROCEDURES

PIM Extraction—The PIM-containing lipidic extract was obtained through purification of the phenolic glycolipids from *M. bovis* BCG 1173P2 (the Pasteur strain) (21) and was briefly summarized in Ref. 1. An acetone-insoluble phospholipids-containing lipid extract was prepared (1) and applied to a QMA-Spherosil M (BioSepra SA, Villeneuve-la-Garenne, France) column that was first irrigated with chloroform, chloroform/methanol (1:1, v/v), methanol in order to elute neutral compounds. Phospholipids were eluted using ammonium acetate containing organic solvents. Indeed, 0.1 M ammonium acetate in chloroform/methanol (1:2, v/v) (fraction A) allowed elution of 750 mg of phospholipids (enriched in phosphatidyl-*myo*-inositol di-mannosides (PIM_2)),and 0.2 M ammonium acetate in chloroform/methanol (1:2, v/v) (fraction B) was subdivided into two fractions. The first volumes allowed elution of 440 mg of phospholipids (cardiolipids essentially), and the next ones allowed elution of 160 mg of phospholipids (mixture of phosphatidyl-*myo*-inositol dimannosides (PIM_2) and hexamannosides (PIM_6)), and finally, 0.2 M ammonium acetate in methanol (fraction C) allowed elution of 55 mg of phospholipids (enriched in PIM_6). Repeated lyophilizations were necessary to eliminate ammonium acetate salts. PIM from *M. smegmatis* (ATCC 607) and *M. tuberculosis* H37Rv (ATCC 27294) were also analyzed.[2]

Purification of the PIM Acyl Forms—Fraction C (20 mg) was loaded in 0.1 M ammonium acetate solution containing 15% (v/v) propanol-1 to octyl-Sepharose CL-4B (Amersham Biosciences) column (20 × 1.5 cm) pre-equilibrated with the same buffer. The column was first eluted with 50 ml of equilibration buffer and then with a linear propanol-1 gradient from 15 to 65% (v/v) (250 ml each) in 0.1 M ammonium acetate solution at a flow rate of 5 ml/h. The fractions were collected every 30 min. 20 μl of each fraction was dried and submitted to acidic hydrolysis (100 μl of trifluoroacetic acid, 2 M, 2 h at 110 °C). The hydrolysates were dried, reconstituted in water, and then analyzed by high pH anion exchange chromatography for mannose content giving the presented chromatogram (Fig. 2*A*). Fractions were pooled according to the purification profile, and repeated lyophilizations were performed to eliminate ammonium acetate salts. An acetone precipitation step was done on each fraction in order to eliminate contaminants issued from the propanol-1. Finally, 1.2 (fraction I), 1 (fraction II), 7.5 (fraction III), and 3 mg (fraction IV) were obtained.

Purification was checked by TLC on aluminum-backed plates of silica gel (Alugram Sil G, Macherey-Nagel, Duren, Germany), using chloroform/methanol/water, 60:35:8 (v/v/v), as migration solvent. A sulfuric anthron spray and a Dittmer-Lester spray were used to detect carbohydrates containing lipids and phosphorus-containing lipids, respectively.

[2] M. Gilleron, V. F. J. Quesniaux, and G. Puzo, unpublished data.

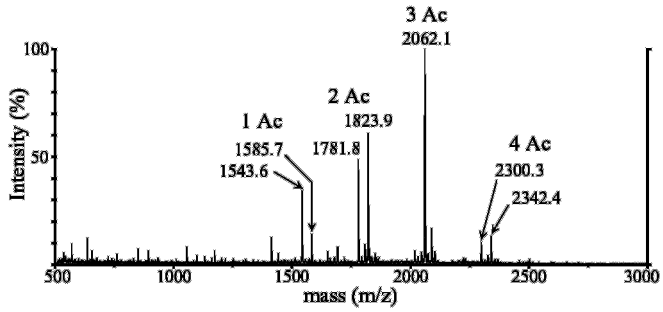

FIG. 1. **Negative MALDI mass spectrum of the PIM_6-enriched fraction C from *M. bovis* BCG, containing 1, 2, 3, and 4 fatty acyl appendages.**

Acetolysis Procedure—200 μg of PIM were treated with 200 μl of anhydrous acetic acid-d_4/acetic anhydride-d_6, 1:1 (v/v), at 110 °C for 12 h. The reaction mixture was dried under stream of nitrogen and was submitted to acetylation. The mixture was dissolved in acetic anhydride/anhydrous pyridine, 1:1 (v/v), at 80 °C for 2 h. The reaction mixture was dried under stream of nitrogen. 20 μl of chloroform/methanol, 9:1 (v/v), was added and analyzed in MALDI-*Tof*-MS in positive and negative modes.

Matrix-assisted Laser Desorption/Ionization-Mass Spectrometry (MALDI-Tof-MS)—Analysis by MALDI-*Tof*-MS was carried out on a Voyager DE-STR (PerSeptive Biosystems, Framingham, MA) using the reflectron mode. Ionization was effected by irradiation with pulsed UV light (337 nm) from an N_2 laser. PIM were analyzed by the instrument operating at 20 kV in the negative ion mode using an extraction delay time set at 200 ns. Typically, spectra from 100 to 250 laser shots were summed to obtain the final spectrum. All of the samples were prepared for MALDI analysis using the on-probe sample cleanup procedure with cation-exchange resin (22). The HABA matrix (from Sigma) was used at a concentration of ~10 mg/ml in ethanol/water (1:1, v/v). Typically, 0.5 μl of PIM sample (10 μg) in a $CHCl_3/CH_3OH/H_2O$ solution and 0.5 μl of the matrix solution, containing ~5–10 cation exchange beads, were deposited on the target, mixed with a micropipet, and dried under a gentle stream of warm air. The measurements were externally calibrated at two points with PIM.

NMR Analysis—NMR spectra were recorded with an Avance DMX500 spectrometer (Bruker GmbH, Karlsruhe, Germany) equipped with an Origin 200 SGI using Xwinnmr 2.6. Samples were dissolved in $CDCl_3/CD_3OD/D_2O$, 60:35:8 (v/v/v), and analyzed in 200 × 5-mm 535-PP NMR tubes at 308 K. Proton chemical shifts are expressed in ppm downfield from the signal of the chloroform (δ_H/TMS 7.27 and δ_C/TMS 77.7). The one-dimensional phosphorus (^{31}P) spectra were measured at 202 MHz with phosphoric acid (85%) as external standard (δp 0.0). All the details concerning NMR sequences used and experimental procedures were detailed in previous study on PIM_2 (1).

Primary Macrophage Cultures—TLR2- and/or TLR4-deficient mice obtained by inter-cross from TLR4-deficient mice (23) and TLR2-deficient mice (24), TLR6-deficient mice (25) and MyD88-deficient mice (26), and their control littermates were bred under specific-pathogen-free conditions in the Transgenose Institute animal breeding facility (Orléans, France). Murine bone marrow cells were isolated from femurs and cultivated (10^6/ml) for 7 days in Dulbecco's minimal essential medium supplemented with 20% horse serum and 30% L929 cell-conditioned medium (as source of M-CSF, as described in Ref. 27). Three days after washing and re-culturing in fresh medium, the cell preparation contained a homogenous population of macrophages. The bone marrow-derived macrophages were plated in 96-well microculture plates (at 10^5 cells/well) and stimulated with LPS (*Escherichia coli*, serotype O111:B4, Sigma, at 100 ng/ml), bacterial lipopeptide (Pam_3-Cys-Ser-Lys_4, EMC microcollections; at 0.5 μg/ml), or PIM preparations at the indicated concentration. Lyophilized PIM preparations were solubilized in Me_2SO and added in the cultures at a non-cytotoxic final concentration of 1–1.5% Me_2SO (cell viability monitored by 3-(4,5-dimethylthiazol-2-yl)-2,5-diphenyltetrazolium bromide assay).

Alternatively the macrophages were infected with *M. bovis* BCG (Pasteur strain 1173P2; kind gift from G. Marchal, Pasteur Institute, Paris, France; at a multiplicity of infection of 2 bacteria per cell). After 18 h of stimulation, the supernatants were harvested and analyzed for cytokine content using commercially available enzyme-linked immunosorbent assay reagents for TNF-α and IL-12p40 (Duoset R & D Systems, Abingdon, UK).

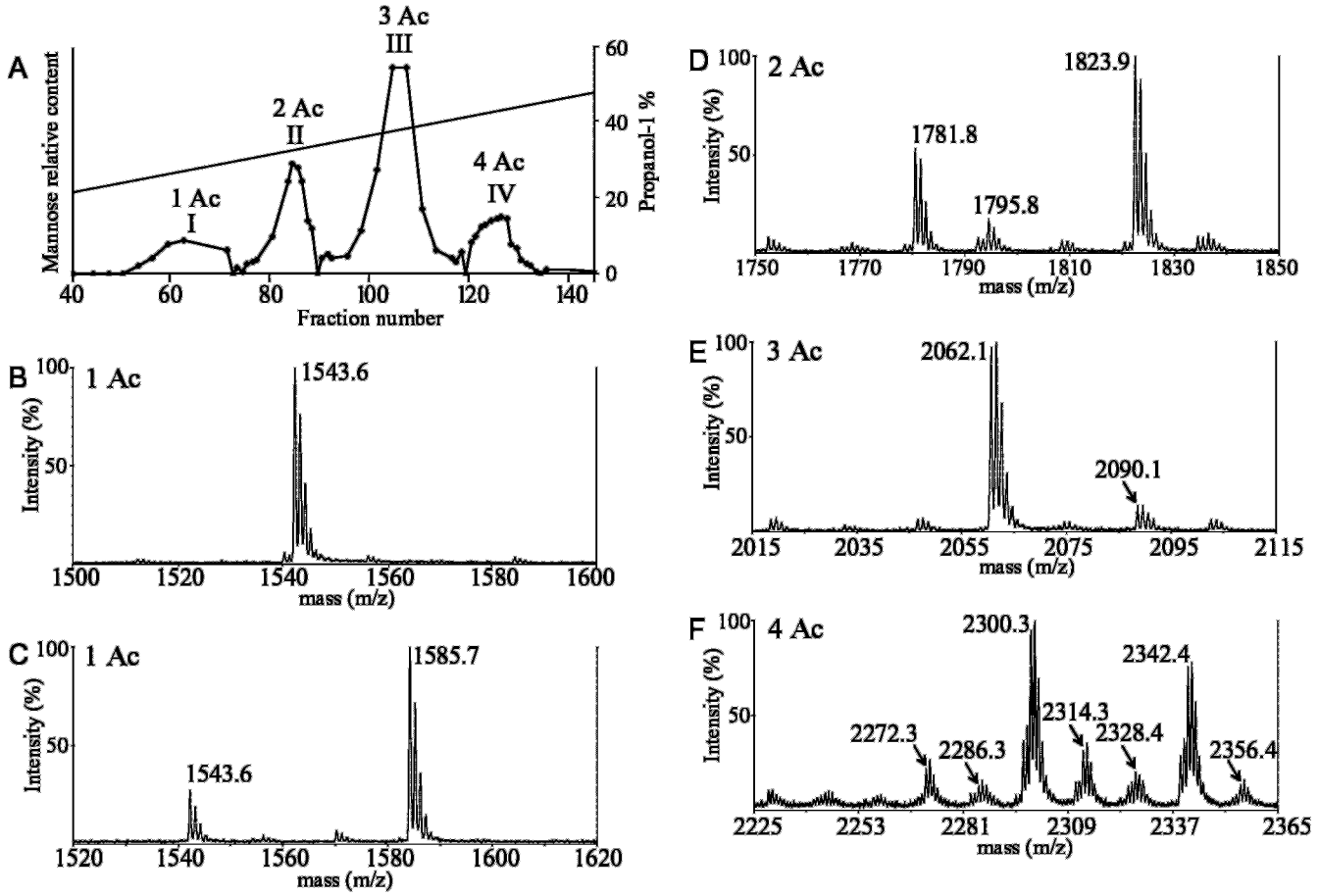

FIG. 2. *A*, octyl-Sepharose chromatography of the PIM_6-enriched fraction C from *M. bovis* BCG. The column was eluted with a propanol-1 linear gradient (15–65% (v/v)) in 0.1 M ammonium acetate. Fractions were analyzed by high pH anion exchange chromatography for their mannose content. *B–F*, negative MALDI mass spectra of the fractions I–IV of the octyl-Sepharose chromatography. Fatty acyl compositions were based on the most abundant fatty acyl chains found by gas chromatography-mass spectrometry analysis, *i.e.* palmitate (C_{16}), tuberculostearate (C_{19}), and for a lesser extent stearate (C_{18}) and heptadecanoate (C_{17}). *B* and *C*, fraction I corresponded to mono-acylated forms, acylated by $1C_{16}$ (*m/z* 1543.6) or $1C_{19}$ (*m/z* 1585.7) (*a*, fraction Ia corresponded to fraction 52 of the octyl-Sepharose, and *b*, fraction Ib corresponded to fraction 62 of the octyl-Sepharose). *D*, fraction II corresponded to di-acylated forms, acylated by $2C_{16}$ (*m/z* 1781.8) and C_{16},C_{19} (*m/z* 1823.9) and in a minor part by C_{16},C_{17} (*m/z* 1795.8). *E*, fraction III corresponded to tri-acylated forms, acylated predominantly by $2C_{16}$,$1C_{19}$ (*m/z* 2062.1), and in a minor part by C_{16},C_{18},C_{19} (*m/z* 2090.1). *F*, fraction IV corresponded to tetra-acylated forms, acylated predominantly by $3C_{16}$,$1C_{19}$ (*m/z* 2300.3) and $2C_{16}$,$2C_{19}$ (*m/z* 2342.4). The ions at *m/z* 2314.3 corresponded to PIM_6 esterified by $2C_{16}$,$2C_{18}$. Minor ions at *m/z* 2272.3, 2286.3, 2328.4, and 2356.4 were attributed to PIM_6 esterified by $3C_{16}$,$1C_{17}$, $3C_{16}$,$1C_{18}$, $2C_{16}$,$1C_{18}$,$1C_{19}$, and $1C_{16}$,$2C_{18}$,C_{19} or $1C_{16}$, $1C_{17}$,$2C_{19}$, respectively. Species esterified by unsaturated fatty acids were also present as each peak consisted of a −2 analog.

RESULTS

Purification of the PIM$_6$ Acyl Forms from M. bovis BCG—An enriched fraction of phosphatidyl-*myo*-inositol hexamannosides (PIM_6) was purified from *M. bovis* BCG as described previously (fraction C (1)). Briefly, PIM are known to be found in the acetone-insoluble fraction of mycobacterial lipidic extract (28). The contaminating neutral compounds were eliminated by QMA anion exchange chromatography, irrigated with neutral eluents. The phospholipids were then eluted with ammonium acetate-containing organic solvents resulting in three fractions, A–C. These fractions were analyzed by ESI-MS in negative mode (1) and revealed that fraction A mainly includes PIM_2 containing a total of three and four fatty acids in addition to phosphatidyl-*myo*-inositol; fraction B contains PIM_2 and PIM_6 containing a total of three and four fatty acids, and fraction C mainly contains the different acyl forms of PIM_6. Fig. 1 presents the negative MALDI spectrum of *M. bovis* BCG fraction C that is dominated by peaks assigned to deprotonated molecular ions $(M - H)^-$ revealing the different acyl forms of PIM_6 present in this fraction. From the predominant fatty acids deduced from gas chromatography-mass spectrometry analysis (not shown), *i.e.* palmitic (C_{16}), tuberculostearic (C_{19}), and stearic (C_{18}) acids and in minor amounts heptadecanoic acids (C_{17}), the fatty acid composition of each acyl form was determined. We then confirmed mono-acylated forms (1Ac) with C_{16} (*m/z* 1543.6) or C_{19} (*m/z* 1585.7), di-acylated forms (2Ac) with $2C_{16}$ (*m/z* 1781.8) or $1C_{16}$,$1C_{19}$ (*m/z* 1823.9), tri-acylated forms (3Ac) mainly with $2C_{16}$,$1C_{19}$ (*m/z* 2062.1), and tetra-acylated forms (4Ac) mainly constituted by $3C_{16}$,$1C_{19}$ (*m/z* 2300.3) or $2C_{16}$,$2C_{19}$ (*m/z* 2342.4). *M. tuberculosis* H37Rv was found to produce as major PIM families PIM_2 and PIM_6 in the same acyl forms as the ones described for *M. bovis* BCG (not shown).

To proceed in the separation of the acyl forms, 20 mg of fraction C were applied on an octyl-Sepharose column, using propanol-1 as eluent (Fig. 2*A*). The different acyl forms were eluted at concentrations of propanol-1 ranging from 25 to 50% and separated into 4 sub-fractions according to the profile elution determined by the mannose content. Each sub-fraction (I to IV) was collected and analyzed by negative MALDI-*Tof*-MS.

MALDI-Tof-MS Characterization of the Octyl-Sepharose Column Fractions—The mass spectra of the fraction I (Fig. 2, *B–C*) revealed that it contained mono-acylated forms of the mole-

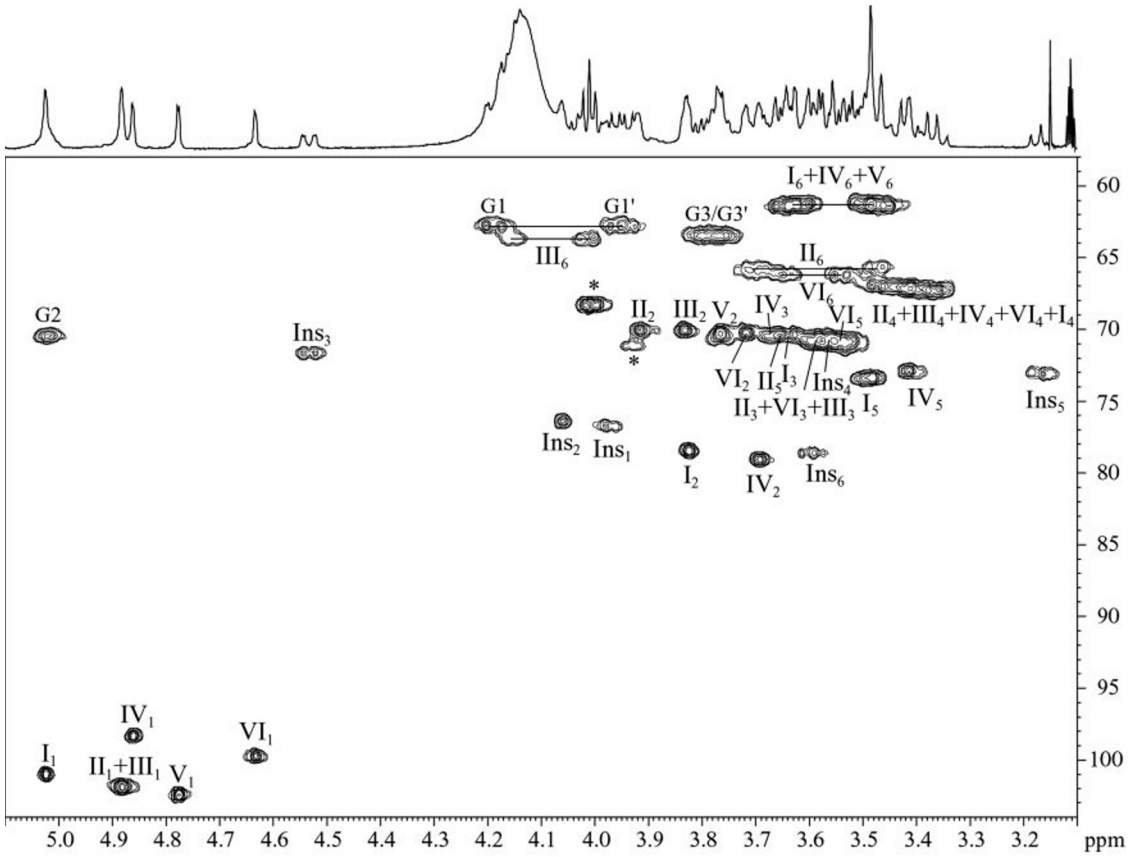

FIG. 3. **^{1}H-^{13}C HMQC spectrum of the tetra-acylated forms.** Fraction IV of the octyl-Sepharose chromatography of the PIM_6 was dissolved in $CDCl_3/CD_3OD/D_2O$, 60:35:8 (v/v/v), and the NMR experiment was realized at 308 K. Mannose units are labeled from I to VI; *numbers with Ins* correspond to the proton number of the *myo*-Ins unit, *and numbers with letter G* correspond to the proton number of the glycerol unit.

cules (1Ac). Indeed, the analysis of fraction Ia revealed deprotonated molecular ions at *m/z* 1543.6 characterizing mono-acylated forms with C_{16} (Fig. 2*B*), whereas mono-acylated forms with C_{19} appeared more abundant in fraction Ib (*m/z* 1585.7) (Fig. 2*C*). The mass spectrum corresponding to fraction II showed three peaks with an intensity above 10% and were assigned to $(M - H)^-$ ions of di-acylated forms: two major peaks at *m/z* 1781.8 and 1823.9 and one minor one at *m/z* 1795.8 (Fig. 2*D*). The two major peaks were characterized as $(M - H)^-$ ions of di-acylated forms containing $2C_{16}$ and $1C_{16}$,$1C_{19}$, respectively, and the minor peak corresponded to $(M - H)^-$ ions of the molecules acylated by $1C_{16}$,$1C_{17}$. The mass spectrum of fraction III (Fig. 2*E*) revealed two peaks of intensity superior to 10% assigned to tri-acylated forms of the molecules. The major peak at *m/z* 2062.1 was attributed to $(M - H)^-$ ions corresponding to tri-acylated forms containing $2C_{16}$,$1C_{19}$, whereas the minor one at *m/z* 2090.1 contains $1C_{16}$,$1C_{18}$, and $1C_{19}$. The mass spectrum of fraction IV appeared more complex, constituted by a series of peaks (Fig. 2*F*) between *m/z* 2230.2 and 2356.4 and assigned to $(M - H)^-$ ions of different tetra-acylated forms. Indeed, the most abundant $(M - H)^-$ ions at *m/z* 2300.3 and 2342.4 characterized tetra-acylated forms containing $3C_{16}$,$1C_{19}$ and $2C_{16}$,$2C_{19}$, whereas the ions at *m/z* 2314.3 corresponded to tetra-acylated forms containing $2C_{16}$,$2C_{18}$. Minor ions at *m/z* 2272.3, 2286.3, 2328.4, and 2356.4 were attributed to the molecules esterified by $3C_{16}$,$1C_{17}$, $3C_{16}$,$1C_{18}$, $2C_{16}$,$1C_{18}$,$1C_{19}$, and $1C_{16}$,$2C_{18}$,$1C_{19}$ or $1C_{16}$ and $1C_{17}$,$2C_{19}$, respectively. In addition, species esterified by unsaturated fatty acids were also present as each peak consisted of a −2 analog.

Therefore, we have developed a powerful preparative method of fractionation, leading to the purification of four purified PIM_6, corresponding to mono-, di-, tri-, and tetra-acyl forms. The structural analysis is further detailed below for the most complex entities, tri- and tetra-acyl forms.

Glycosidic Analysis of Native Tetra-acyl Forms—The sequence of glycosyl residues in PIM_6 was established using a range of high resolution NMR techniques applied to the tetra-acylated molecules. The ^{1}H NMR spectrum of the native molecules in $CDCl_3/CD_3OD/D_2O$, 60:35:8 (v/v/v), at 500 MHz showed a complex anomeric proton region (between 4.4 and 5.1 ppm) (Fig. 3). Anomeric signals were investigated thanks to the ^{1}H-^{13}C HMQC spectrum (Fig. 3). Indeed, from the protons resonating between 4.4 and 5.1 ppm, two of them correlated with carbons out of the anomeric zone: proton at δ 5.02 correlated with a carbon at 70.6 ppm and proton at δ 4.53 correlated with a carbon at 71.7 ppm. From previous studies (1, 2), they were respectively assigned to H2 of Gro and H3 of *myo*-Ins. These protons are deshielded due to the presence of gem acyl group. Moreover, the coupling constants measured on the proton at δ 4.53 ($J_{2,3}$ 2.4 Hz and $J_{3,4}$ 10.6 Hz) confirmed its attribution to *myo*-Ins H3. The other proton resonances correlating with carbons resonating around 100 ppm accounted for the six mannose units labeled from I to VI in decreasing order of their chemical shifts. Indeed, integration of the anomeric signals (H1) proved that the signal resonating at 4.88 ppm corresponded to two protons (II_1 and III_1). The α-anomeric configuration of the mannoses was deduced from the values of the one bound coupling constant ($^1J_{C1,H1}$) above 170 Hz, measured on non-decoupled ^{1}H-^{13}C HMQC spectrum (not shown).

The H2 protons of each α-Man*p* unit was determined using the COSY spectrum (Fig. 4*A*) although H2 of system I was partly hidden by the H3/H3′ of glycerol (Gro). The entire spin system of Gro can be analyzed from the COSY spectrum (Fig.

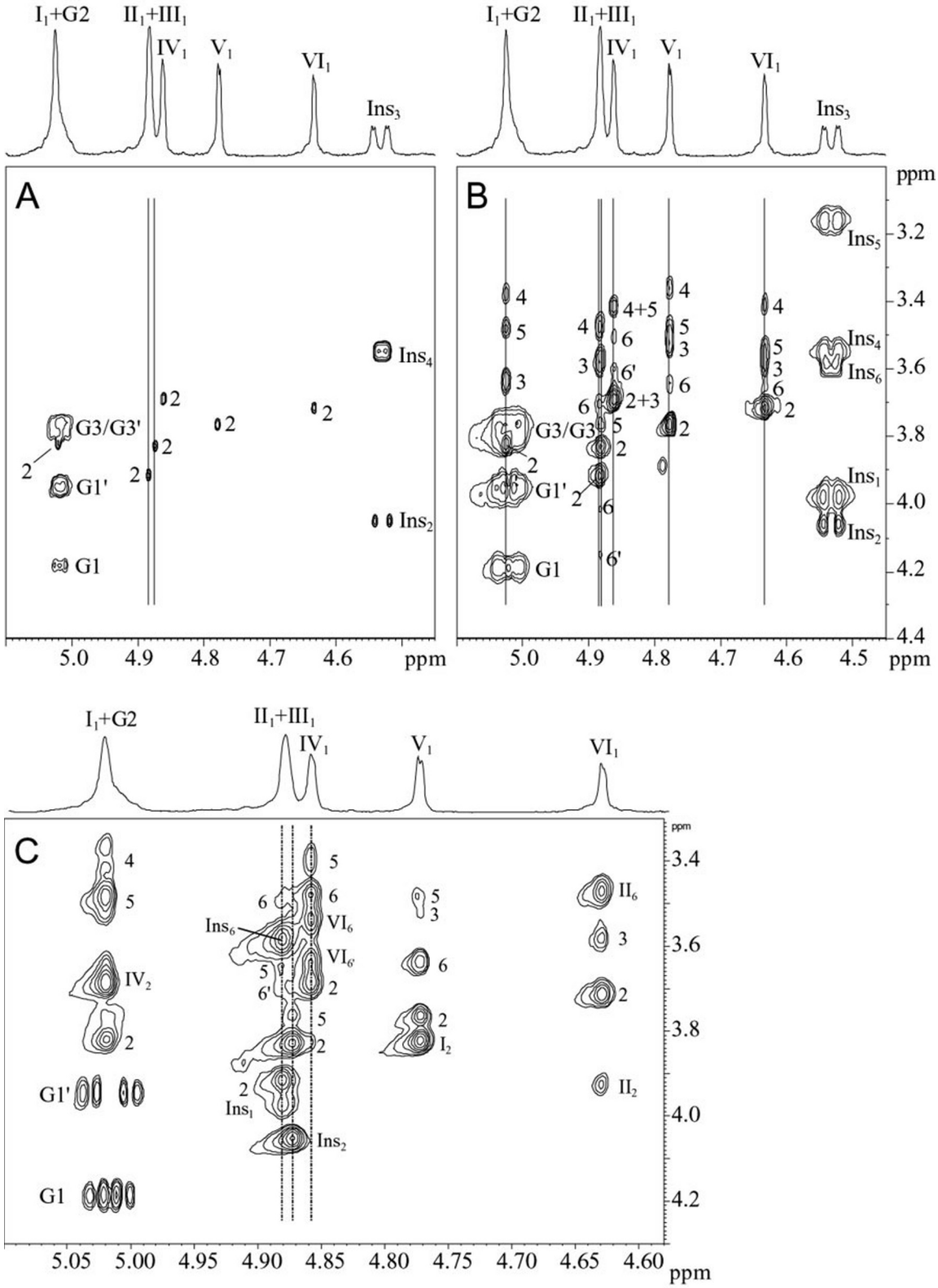

FIG. 4. **Expanded region (δF_2 4.45–5.1 and δF_1 3.0–4.4) of the ^{1}H-^{1}H COSY (*A*), HOHAHA (*B*), and (δF_2 4.45–5.1 and δF_1 3.0–4.4) of the ^{1}H-^{1}H ROESY (*C*) spectra of the tetra-acylated forms at 308 K.** The product was dissolved in $CDCl_3/CD_3OD/D_2O$, 60:35:8 (v/v/v). Mannose units are labeled from I to VI; *numbers with Ins* correspond to the proton number of the *myo*-Ins unit, and *numbers with letter G* correspond to the proton number of the glycerol unit. *C*, intra-residual contacts are expressed only with a *number,* whereas inter-residual contacts are expressed with the *roman number* of the concerned unit followed by the number corresponding to the proton number of the unit.

4*A*) and those of the *myo*-Ins from the HOHAHA spectrum (Fig. 4*B*). The six mannose spin systems could be completely assigned (Table I) using ^{1}H-^{1}H HOHAHA (Fig. 4*B*) and ^{1}H-^{13}C HMQC (Fig. 3). The deshielded values of the chemical shifts of the C2 of units I (δ 78.5) and IV (δ 79.1) and of C6 of units II (δ 65.8) and VI (δ 66.3) revealed the sites of glycosylation of the concerned units. The absence of deshielding concerning the carbons of systems III and V indicated that these units III and

TABLE I
^{1}H and ^{13}C NMR chemical shifts of the tetra-acylated forms measured at 308 K in $CDCl_3/CD_3OD/D_2O$, 60:35:8, v/v/v

	1	2	3	4	5	6	Conclusion
I	5.02	3.83	3.64	3.39	3.48	3.47/3.64	2-*O*-Linked
	101.0	*78.5*	70.4	67.3	73.4	61.5	
II	4.88	3.92	3.60	3.49	3.65	3.48/3.70	6-*O*-Linked
	101.8	70.1	70.9	67.0	70.5	*65.8*	
III	4.88	3.84	3.58	3.47	3.78	4.02/4.15	Terminal, 6-*O*-Acylated
	101.8	70.1	70.8	67.1	70.7	63.9	
IV	4.86	3.70	3.68	3.42	3.42	3.51/3.60	2-*O*-Linked
	98.3	*79.1*	70.5	67.3	73.0	61.4	
V	4.78	3.78	3.53	3.37	3.50	3.47/3.65	Terminal
	102.3	70.4	71.0	67.4	71.0	61.5	
VI	4.63	3.72	3.59	3.42	3.55	3.54/3.65	6-*O*-Linked
	99.7	70.3	70.8	67.3	70.9	*66.3*	
myo-Ins	3.97	4.06	4.53	3.55	3.17	3.60	3-*O*-Acylated
	76.8	76.5	71.7	70.9	73.1	78.7	
Gro	4.19/3.95	5.02	3.79/3.76				1,2-Di-*O*-Acylated
	62.9	70.6	63.6				

V were terminal. The chemical shift of the C6 of unit III (δ 63.9) (Table I) was intermediate between those of the C6 of units I, IV, and V (around 61.5 ppm) that were not glycosylated in C6 and those of the C6 of units II and VI (around 66.0) that were glycosylated in C6. Moreover, H6/H6′ protons of unit III were deshielded (4.02:4.15) (Table I). Thus, these data demonstrated that this unit is acylated in position 6.

The glycosidic sequence was next deduced from the inter-residual nuclear Overhauser effect contacts observed in the ^{1}H-^{1}H ROESY spectrum (Fig. 4*C*). This sequence was used here to observe short through space connectivities between the anomeric proton of each mannose and the proton of the adjacent glycosidically linked residue. The anomeric proton of spin system I (δ 5.02) correlated with H2 of system IV, indicating that α-Man*p* unit I is linked to the C2 position of α-Man*p* unit IV. In the same way, the occurrence of cross-peaks relating H1 (IV)/H6 (VI), H1 (V)/H2 (I), and H1 (VI)/H6 (II) established the partial linear sequence V-(1→2)-I-(1→2)-IV-(1→6)-VI-(1→6)-II. Anomeric protons of α-Man*p* units II and III were then separated showing both correlations with protons belonging to the Ins unit.

The H1 of system III showed a nuclear Overhauser effect contact with proton 2 of *myo*-Ins, revealing that this unit is linked in position 2 of the *myo*-Ins. The H1 of system II showed two cross-peaks with protons 1 and 6 of *myo*-Ins. As explained below, two-dimensional ^{1}H-^{31}P HMQC analysis allowed us to define one of the positions of substitution of the phosphorus as position 1 of the *myo*-Ins. Thus, system II was deduced to be linked in position 6 of the *myo*-Ins.

Therefore, the glycosidic analysis of the tetra-acylated form of the molecules using a combination of scalar and dipolar homonuclear and heteronuclear NMR sequences demonstrated the structure t-α-Man*p*-(1→2)-α-Man*p*-(1→2)-α-Man*p*-(1→6)-α-Man*p*-(1→6)-α-Man*p*-(1→6)-*myo*-Ins-(2←1)-t-α-Man*p*, as depicted in Fig. 5.

Anchor Structure of Native Tetra-acyl Forms—The NMR strategy developed to study PIM_2 containing a total of 4 fatty acids (1) was used here. From the ^{1}H-^{31}P HMQC experiment, the prochiral H-3 and H-3′ Gro protons and the *myo*-Ins H-1 were easily assigned (not shown). The remaining *myo-Ins* and Gro protons were then observed on the two-dimensional ^{1}H-^{31}P HMQC-HOHAHA spectrum (Fig. 6*B*) and were assigned from their multiplicity and chemical shifts (29) and with the help of the ^{1}H-^{1}H HOHAHA spectrum (Fig. 6, *C–D*). The different chemical shifts typified the presence or absence of an acyl appendage. The chemical shifts of the H-1 (4.19/3.95 ppm) and H-2 (5.02 ppm) revealed a di-acyl-Gro (29). The downfield shift of the *myo*-Ins H-3 resonating at 4.53 ppm then signed the C3 acyl appendage. A fourth position of acylation, the C6 of the Man*p*, could be assigned by analysis of the two-dimensional ^{1}H-^{13}C HMQC spectrum. Indeed, the chemical shifts of H-6/H-6′ of α-Man*p* unit III (4.02/4.15 ppm) proved that this position is also acylated. The slight deshielding of C6 resonance (from 61.5 to 63.9 ppm) confirmed this assignment.

Therefore, the analytical approach applied to this acyl form of PIM_6 (containing four fatty acids in total) revealed that the four positions of acylation were the same as the ones described in case of the corresponding acyl form of PIM_2 (1): the positions C1 and C2 of the Gro, position C3 of the *myo*-Ins unit, and position C6 of the Man*p* unit linked to C2 of the *myo*-Ins.

Acyl Distribution of Native Tetra-acyl Forms—The nature of the fatty acids esterifying the different sites was investigated by mass spectrometry using MALDI-*Tof*-MS analysis of the acetolysis reaction products of the native tetra-acyl forms of the molecules (not shown). Acetolysis cleaves the phosphoglycerol linkage without altering the fatty acid esters, leading to two entities: the hexamannosyl-inositol phosphate moiety (Man_6-Ins-P) and the acyl-glycerol residue, as already described in Ref. 1. The hexamannosyl-inositol phosphate moiety was observed in negative mode as $[M - H]^-$ ions, whereas the acyl-glycerol part was analyzed in positive mode as $[M + Na]^+$ ions. As described previously, the acetolysis reaction produces two populations of Man_6-Ins-P moieties that differ by the presence or absence of an acetyl group on the phosphate (1). But as this acetate present on the phosphate is very labile (mixed anhydride), it is partially hydrolyzed when the sample is mixed with the matrix (HABA diluted in $EtOH/H_2O$). To discriminate between acetate groups and changes of C19 by C16, the reaction was made with perdeuterated acetic acid and acetic anhydride.

The positive MALDI-*Tof*-MS spectrum of the perdeutero-acetolyzed of the tetra-acylated molecules showed an intense peak at *m/z* 678.6 assigned to sodium adduct of the di-acylated C_{16}/C_{19} Gro (not shown). The negative mass spectrum mainly showed two peaks at *m/z* 2653.7 and 2695.8 corresponding to the Man_6-Ins-P moiety acylated with $2C_{16}$ and C_{16},C_{19}, respectively. Less intense peaks were also observed corresponding to the Man_6-Ins-P moiety acylated with other combinations of fatty acids. Taken together, these results indicate that the glycerol is always acylated by C_{16},C_{19}, and we can postulate that the mannose is acylated by a C_{16}, whereas the nature of the fatty acid present on the inositol is variable, being predominantly C_{16} or C_{19}.

Analysis of Native Tri-acyl Forms—^{1}H-^{13}C HMQC spectrum of the tri-acylated molecules exhibited the same cross-peaks as for the tetra-acylated one, except for the inositol spin system defined as δ H1/C1 3.93/70.64, δ H2/C2 4.04/78.68, δ H3/C3 3.27/70.63, δ H4/C4 3.36/67.63, δ H5/C5 3.10/73.68, and δ H6/C6 3.60/79.03, indicating that there is no fatty acyl append-

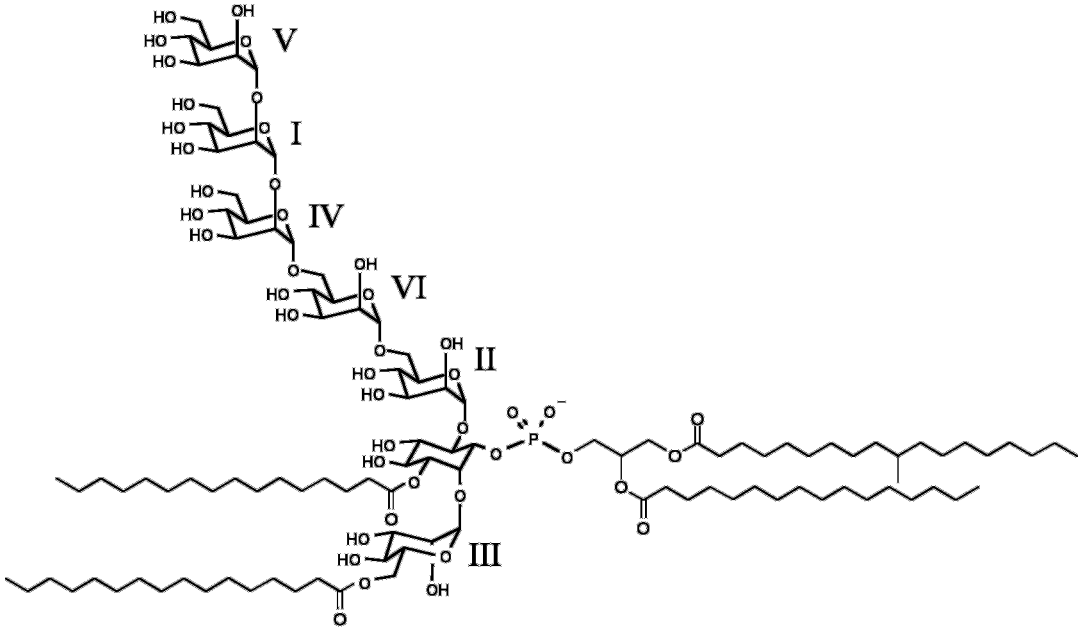

FIG. 5. **Structural model of PIM$_6$ acylated by four fatty acids in total, here 3C$_{16}$/1C$_{19}$.**

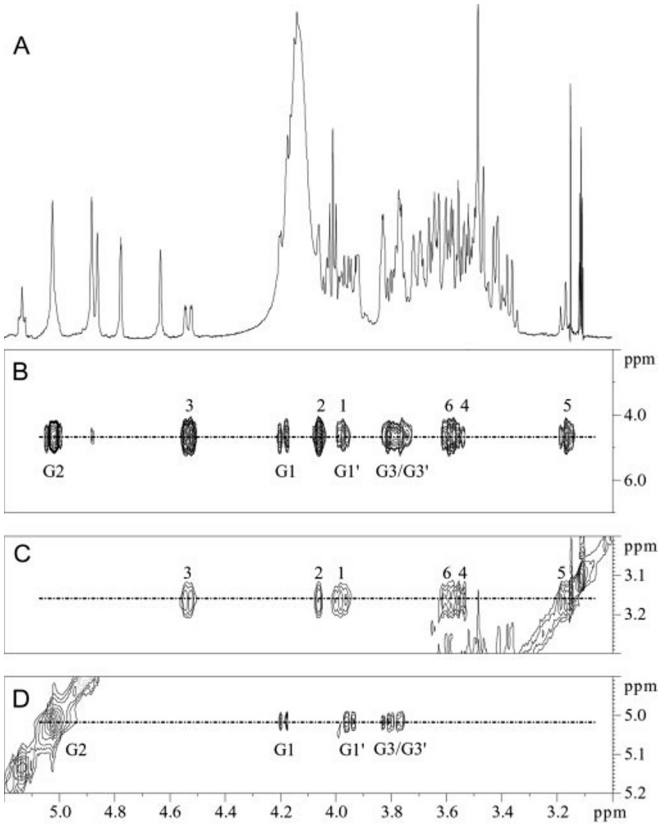

FIG. 6. **NMR analysis of the phosphate substituents of the tetra-acylated forms.** Expanded region (*A*) (δ ^{1}H, 3.00–5.20) of the ^{1}H one-dimensional spectrum. Expanded region (*B*) (δ ^{1}H, 3.00–5.20, and ^{31}P, 2.00–7.00) of the ^{1}H-^{31}P 55 ms HMQC-HOHAHA spectrum. Expanded zone (*C*) (δ ^{1}H, 3.00–5.20 and 3.00–3.30) of the two-dimensional ^{1}H-^{1}H HOHAHA spectrum showing the *myo*-Ins spin systems. Expanded zone (*D*) (δ ^{1}H, 3.00–5.20 and 4.90–5.20) of the two-dimensional ^{1}H-^{1}H HOHAHA spectrum showing the Gro spin systems. The product was dissolved in $CDCl_3/CD_3OD/D_2O$, 60:35:8 (v/v/v), and all NMR experiments were realized at 308 K.

age on C3. The three fatty acids were found on both positions of Gro and on the α-Man*p* unit on the C2 of *myo*-Ins. The positive MALDI-*Tof*-MS spectrum of deutero-acetolyzed molecules showed a similar intense peak at *m/z* 678.6 assigned to the sodium adduct of the di-acylated C$_{16}$/C$_{19}$ Gro as the one observed in the case of the tetra-acylated molecules (not shown). The negative mass spectrum mainly showed one peak at *m/z* 2460.5 corresponding to the Man$_6$-Ins-P moiety acylated with one 1C$_{16}$. Thus, the results indicate that the tri-acylated molecules predominantly exist with 2C$_{16}$ and 1C$_{19}$, in agreement with the negative MALDI-*Tof* analysis of the native molecules (Fig. 2*E*), the glycerol being di-acylated by C$_{16}$/C$_{19}$ and the mannose bearing a C$_{16}$.

Macrophage Stimulation by PIM$_2$ and PIM$_6$—Unfractionated PIM have been shown to stimulate the murine RAW 264.7 monocytic cell line to produce TNF-α (15), and we asked whether purified PIM$_2$ and PIM$_6$ were equally pro-inflammatory. First, unfractionated PIM$_2$ preparation was tested and shown to stimulate TNF-α and IL-12 p40 secretion by primary murine macrophages (not shown). Then two different well defined acyl forms of PIM$_2$ were assayed as follows: a fraction (F6) containing lyso-PI and lyso-PIM$_2$ (both containing C$_{16}$) and a fraction (F7) containing more acylated forms of PIM$_2$ (tri-acylated and tetra-acylated molecules). Both PIM$_2$ fractions induced TNF-α secretion irrespective of their acyl forms (Fig. 7). The concentration of TNF-α secreted was clearly sub-maximal (~1 ng/ml) as compared with those achieved by stimulation with strong stimuli such as LPS or BLP or after infection with live BCG (~15 ng/ml; Fig. 7*A*). We next asked whether PIM$_6$ exhibited a similar function. The unfractionated PIM$_6$ preparation (F1) also stimulated TNF-α secretion by macrophages (Fig. 7*B*). To determine whether the number of fatty acids played a role in the stimulation of TNF-α secretion, the purified acyl forms of PIM$_6$ (F2 to F5) were tested for their capacity to stimulate macrophages to produce TNF-α. No clear enrichment in stimulatory activity was observed with the purified PIM$_6$ acylated forms (mono- to tetra-acylated molecules) as compared with the unfractionated PIM$_6$ (Fig. 7*B*). Only marginal levels of IL-12p40 were detected after incubation of macrophages with PIM$_2$ or PIM$_6$ (data not shown).

Thus, both PIM$_2$ and PIM$_6$ stimulated TNF-α secretion by primary macrophages, and this activity seemed independent from the number and the nature of the PIM$_2$ and PIM$_6$ acyl moieties.

TLR Dependence of PIM Activity—The unfractionated PIM

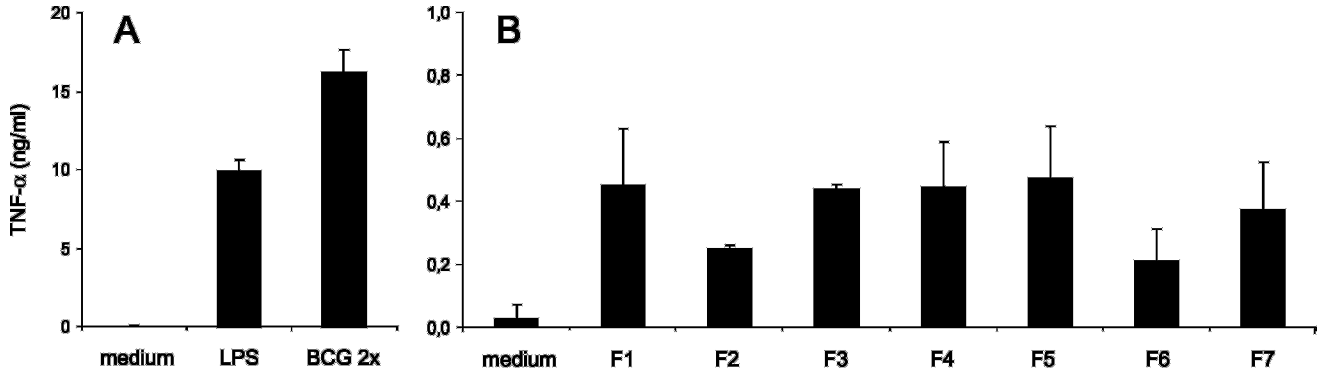

FIG. 7. **Induction of TNF-α by primary macrophages stimulated with BCG or PIM_2- and PIM_6-purified fractions.** Murine bone marrow-derived macrophages were infected for 24 h with BCG (at a multiplicity of infection of 2; *A*) or incubated with PIM_6 and PIM_2 fractions (F1 to F7) (all PIM fractions at 30 μg/ml; *B*). *F1* corresponds to the PIM_6 family, *i.e.* a fraction containing all the acyl forms. *F2, F3, F4,* and *F5* correspond to mono- (Ac1), di- (Ac2), tri- (Ac3), and tetra-acylated (Ac4) forms, respectively; *F6*, a fraction containing lyso-PI and lyso-PIM_2 (both containing C_{16}); *F7*, a fraction containing more acylated forms of PIM_2 (tri-acylated and tetra-acylated molecules). TNF-α was measured in the supernatants. Results are mean ± S.D. from $n = 2$ mice and are from one representative experiment out of two independent experiments.

preparation was shown to be a TLR2 agonist, based on reporter assay with Chinese hamster ovary cell lines transfected with the *tlr2* gene (15). Here bone marrow-derived macrophages prepared from mice rendered deficient for TLR2 and/or TLR4, for TLR6, or for MyD88, the adaptor common to the different TLR, were used to investigate the TLR dependence of the PIM_2 and PIM_6 responses. The macrophages were stimulated with the fraction (F6) containing lyso-PI and lyso-PIM_2 (both containing C_{16}), and the fraction (F7) containing more acylated forms of PIM_2 (tri-acylated and tetra-acylated molecules) or with the PIM_6 fraction (F1) and TNF-α (Fig. 8) and IL-12 p40 (not shown) secretions were assessed. The production of TNF-α by primary macrophages in response to the PIM_2 and PIM_6 fractions is dependent on TLR2, as no TNF-α could be detected in the supernatant of macrophages deficient for TLR2, although cells deficient for TLR4 were efficiently stimulated by these fractions (Fig. 8, *B* and *C*). As expected, no cytokine production was detected in the supernatants of macrophages isolated from the double knock-out mice (TLR2−/− and TLR4−/−) (Fig. 8, *B* and *C*). Thus, PIM_6 are capable of inducing TNF-α secretion via a TLR2-dependent pathway. TLR2 has been shown to heterodimerize with TLR1 or TLR6 (30), and we next looked at the implication of TLR6 in the PIM-TLR2 interaction. TLR6 deficiency did not impair the ability of the macrophages to respond to PIM_2 or PIM_6 (Fig. 8, *D–F*). MyD88 is involved in most of the TLR-mediated signals (31), including TLR2 as shown here for the TLR2 agonist BLP and for the best of the response to the TLR4 agonist LPS (Fig. 8*D*), and we showed that macrophages deficient for MyD88 did not respond to the PIM_2 or PIM_6 stimulation (Fig. 8, *E* and *F*). Thus, both PIM_2 and PIM_6 stimulate TNF-α secretion by macrophages through TLR2 and not TLR4. TLR6 is not essential in this response which involves signaling through the adaptor MyD88.

DISCUSSION

The present study constitutes the first complete structural analysis of the native PIM_6 from *M. bovis* BCG allowing the definition of the structure of the tetra-acylated form of the molecule as depicted in Fig. 5. The saccharidic part is in complete agreement with that proposed in the 1960s (for a review, see Ref. 32) and determined for the deacylated PIM_6 by Severn *et al.* (20). Beyond this, the analysis presented here allows us to discriminate the different structures hiding beneath the term "PIM_6." Indeed, the "PIM_6 family" corresponds to a mixture of 10 or 12 acyl forms. Purification of these different species proved to be crucial for the complete structural study of the native molecules. We developed a rapid and powerful method for allowing us in a first step to separate PIM_2 from PIM_6 using a QMA column and in a second step to separate acyl forms using an octyl-Sepharose column, similar to that used to purify LAM acyl forms, as described by Leopold and Fischer (33) and applied in our laboratory by Nigou *et al.* (34). The purification of the PIM family from *M. bovis* BCG as well as *M. smegmatis* 607 and *M. tuberculosis* H37Rv revealed that very small quantities of intermediate forms (PIM_1, PIM_3, PIM_4, and PIM_5) were found and that the more polar PIM corresponded to PIM_6 and not PIM_5, in contrast to early conclusions (35) and still reported in the literature (5, 7, 36). The purification to homogeneity of the different PIM using isocratic silicic flash chromatography was unsuccessful, except for the PIM_2 containing four fatty acyl appendages in total (2). Indeed, as shown on Fig. 9, the more polar PIM_2 co-migrate with the different acyl forms of PIM_6.

The structural strategy used to characterize PIM_6 acyl forms was similar to the one successfully used to define PIM_2 acyl forms (1) and combines the potency of complementary analytical techniques, NMR and mass spectrometry. NMR was used to characterize the acylation positions, whereas mass spectrometry gave information concerning the number of fatty acids and the nature of the fatty acids present at each position. MALDI or ESI modes were chosen rather than fast atom bombardment, because the molecules could be analyzed without derivatization preventing the loss of any labile substituents. In this study, MALDI-MS was chosen rather than ESI-MS as a same deposit could be analyzed in positive or negative mode. Indeed, concerning the analysis of the acetolysis products, the hexamannosyl-inositol phosphate moiety (Man_6-Ins-P) was observed in negative mode, whereas the acyl-glycerol residue was analyzed in positive mode. The complete NMR study required some milligrams of purified product. This was detailed for the more complex acyl forms, the tri-acylated and the tetra-acylated ones.

The results obtained are summarized in Table II. The mono-acylated forms are identified for lyso-PIM_6 with C_{16} or C_{19} in position 1 of the glycerol. The di-acylated forms appear as two populations almost equally represented as one with $2C_{16}$ and one with $1C_{16}$ and $1C_{19}$, both fatty acids being on the glycerol and structurally corresponding to "true" PIM_6. In contrast, concerning tri-acylated forms, a major acyl form was observed, containing $2C_{16}$ and $1C_{19}$, the glycerol being di-acylated by C_{16},C_{19} and the mannose bearing a C_{16}. They should then correspond to mono-acylated-PIM_6 (or Ac_1PIM_6). Interestingly, the acyl form containing $3C_{16}$ was not observed, indicating that

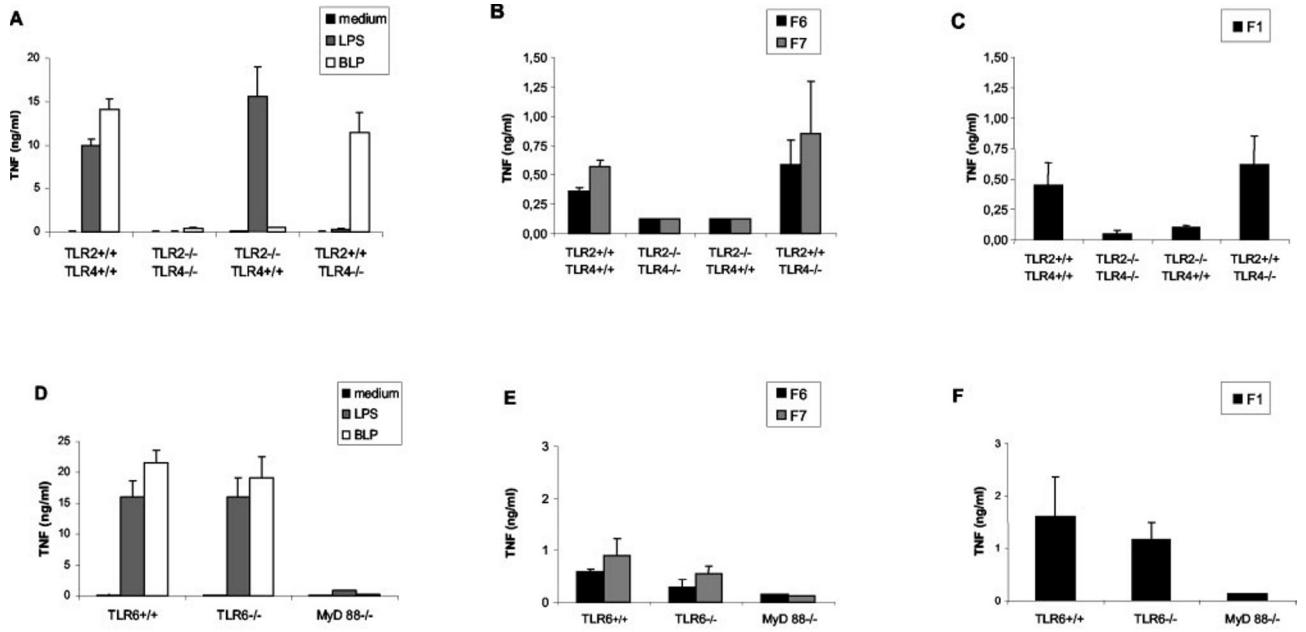

FIG. 8. **TLR dependence of macrophage stimulation by PIM$_6$.** Bone marrow-derived macrophages from mice deficient in TLR2 and/or TLR4 (*A–C*) or deficient for TLR6 or MyD88 (*D–F*) were incubated with the TLR2 agonist BLP (0.5 μg/ml; *A* and *D*), the TLR4 agonist LPS (100 ng/ml; *A* and *D*), with F6 and F7 (20 μg/ml; *B* and *E*), or with F1 (20 μg/ml; *C* and *F*) for 24 h. *F1*, *F6*, and *F7* are defined in the legend of Fig. 7. TNF-α was measured in the supernatants by enzyme-linked immunosorbent assay. Results are mean ± S.D. from $n = 2$ mice per genotype and are from one representative experiment out of two independent experiments.

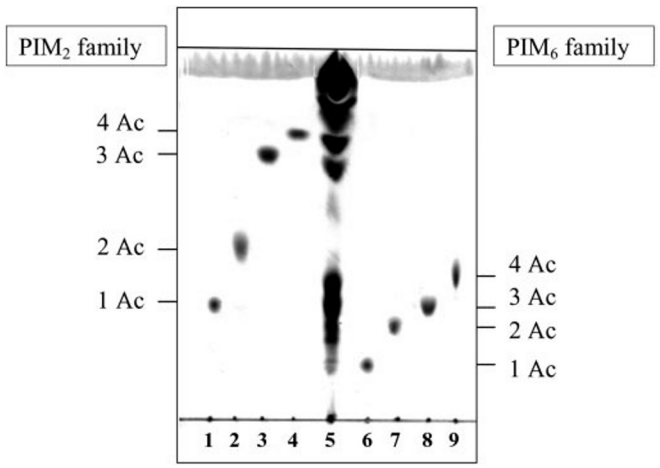

FIG. 9. **TLC analysis of the major PIM purified from *M. bovis* BCG.** *Lanes 1–4*, purified acyl forms of PIM$_2$; *lane 5*, *M. bovis* BCG total lipidic extract; *lanes 6–9*, purified acyl forms of PIM$_6$. TLC was developed with $CHCl_3/CH_3OH/H_2O$, 60:35:8 (v/v/v), and sprayed with orcinol.

the tri-acylated forms arose from the di-acylated forms containing C_{16},C_{19} as fatty acyl appendages. The tetra-acylated forms were present as essentially two populations, $3C_{16}$,$1C_{19}$ or $2C_{16}$,$2C_{19}$. The acylation positions were here clearly elucidated as being both positions of Gro, the C3 of the *myo*-Ins unit and the C6 of the Man*p* linked to the C2 of the *myo*-Ins unit. Taken together, the same conclusions as for the acyl forms of PIM$_2$ could be made. Indeed, the results indicate that the glycerol is preferentially acylated by C_{16},C_{19}. However, the nature of the fatty acid present on the *myo*-inositol appears highly variable, being essentially C_{16} or C_{19}.

As mentioned previously (1), the biosynthetic linkage between PIM$_2$, LM, and LAM appears now to be more and more evident, as the same anchor structures were found for all these lipoglycans. However, even if the acyl forms found for PIM$_6$ were exactly the same as the ones found for PIM$_2$, LM, and LAM, PIM$_6$ are not part of the LM/LAM biosynthetic pathway. Indeed, the linear mannan backbone found in LM and LAM is constituted by a linear α-(1→6)-linked Man*p,* whereas PIM$_6$ exhibit at its extremity α-(1→2) links. PIM$_6$ appears to be an end product and may have a specific role.

Mammalian TLR proteins are pattern recognition receptors for a wide array of bacterial and viral products (17). Gram-negative bacterial lipopolysaccharide (LPS) activates cells through TLR4, whereas the mycobacterial cell wall lipoglycans, AraLAM, activate cells through TLR2. Recently, Jones *et al.* (15) identified a secreted TLR2 agonist activity in short term culture filtrates of *M. tuberculosis*, which they called STF, for "soluble tuberculosis factor." To determine the identity of the TLR2 agonist present in soluble tuberculosis factor, they used preparative SDS-PAGE. The TLR2 agonist activity was present in one fraction, with an apparent molecular size of 6 kDa, raising the possibility that the TLR2 agonist was PIM$_2$. By using TLC, the authors reported the presence of two major species, PIM$_1$ and PIM$_2$. In that case, the precise structure of the TLR2 agonist was not determined. We confirm here that structurally defined acyl forms of PIM$_2$ stimulated TNF-α secretion by primary macrophages in a TLR2-dependent fashion. We then demonstrated that the major polar PIM from *M. bovis* BCG and *M. tuberculosis*, PIM$_6$, also stimulated TNF-α secretion and that this secretion was mediated by TLR2 but not TLR4. TLR2 has been shown to heterodimerize with TLR1 or TLR6 (30). We show here that the TLR2-mediated stimulation of macrophages by PIM$_2$ and PIM$_6$ was independent of TLR6 but that both PIM$_2$ and PIM$_6$ signaled via the adaptor molecule MyD88.

It has been demonstrated in the case of LPS that saturated fatty acids acylated in lipid A moiety are essential for its biological activities. Saturated fatty acids, but not unsaturated fatty acids, induce NF-κB activation and expression of inflammatory markers in macrophages (37). In addition, it has been proposed that the shape of lipid A, influenced by the length and number of acyl chains, asymmetry of acyl groups, and distribution of negative charges, determine the interaction of LPS with different TLR (38). This would explain how *E. coli* LPS, with a strong conical shape lipid A, interact with TLR4,

TABLE II

Major PIM_6 acyl forms evidenced in M. bovis BCG

The relative abundance of the different species for each acyl form was determined from the integration of the corresponding monoisotopic signals in the negative MALDI spectrum of the PIM_6-enriched fraction C from *M. bovis* BCG (Fig. 1).

Acylation degree	*m/z*	Fatty acids nature	Gro		Man*p* 6	*myo*-Ins 3	%	Structure
			1	2				
1	1543.6	C_{16}	C_{16}				70	Lyso-PIM_6
	1585.7	C_{19}	C_{19}				30	
2	1781.8	C_{16},C_{16}	C_{16}	C_{16}			45	PIM_6
	1823.9	C_{16},C_{19}	C_{16}	C_{19}			55	
3	2062.1	$2C_{16}$,C_{19}	C_{16}	C_{19}	C_{16}		100	Ac_1-PIM_6
4	2300.3	$3C_{16}$,C_{19}	C_{16}	C_{19}	C_{16}	C_{16}	45	Ac_2-PIM_6
	2342.4	$2C_{16}$,$2C_{19}$	C_{16}	C_{19}	C_{16}	C_{19}	55	

whereas *Porphyromonas gingivalis* or *Rhodobacter sphaeroides* LPS, with a more cylindrical shape lipid A, are TLR2 agonists (38). Here we asked whether different PIM_2 and PIM_6 acyl forms, bearing 1–4 acyl residues, were equally potent in stimulating macrophages to produce TNF-α. We show that the TNF-α stimulating activity of PIM_6 is independent from the number and the nature of the acyl moieties present on the molecules. This seemed to be also the case for PIM_2 as both mono- (F6) and tri- and tetra-acylated (F7) forms studied here had similar activity.

In infected macrophages, PIM were shown to traffic out of the mycobacterial phagosome among other mycobacterial lipids, such as LAM, and are released to the medium and bystander uninfected cells (14). We show here that both major PIM species from *M. bovis* BCG, *M. smegmatis* 607, and *M. tuberculosis* H37Rv, PIM_2 and PIM_6, are agonists of TLR2, irrespective of their acylation state. ManLAM from slow-growing mycobacteria such as *M. bovis* or *M. tuberculosis* do not show such pro-inflammatory effects or TLR2-dependent activity (39).[2] TLR2 may be present intracellularly, recruited to macrophage phagosomes, where they sample the content of the vacuole, and contribute to elaborate an inflammatory response appropriate for defense against a specific pathogen (40). The trafficking and export of PIM_2 and the more polar PIM_6 from *M. bovis* or *M. tuberculosis* could thus contribute to maintaining the smoldering activation state of the infected macrophage and of the neighboring cells in the tuberculous granuloma through TLR2 activation, and contribute to the innate immunity necessary to contain latent infection.

Acknowledgments—We gratefully acknowledge Dr. J. Nigou (CNRS, Toulouse, France) and Dr. B. Ryffel (CNRS, Orléans, France) for helpful discussions and carefully reading the manuscript.

REFERENCES

1. Gilleron, M., Ronet, C., Mempel, M., Monsarrat, B., Gachelin, G., and Puzo, G. (2001) *J. Biol. Chem.* **276,** 34896–34904
2. Gilleron, M., Nigou, J., Cahuzac, B., and Puzo, G. (1999) *J. Mol. Biol.* **285,** 2147–2160
3. Nigou, J., Gilleron, M., and Puzo, G. (2003) *Biochimie* (*Paris*) **85,** 153–166
4. Khoo, K. H., Dell, A., Morris, H. R., Brennan, P. J., and Chatterjee, D. (1995) *Glycobiology* **5,** 117–127
5. Besra, G. S., Morehouse, C. B., Rittner, C. M., Waechter, C. J., and Brennan, P. J. (1997) *J. Biol. Chem.* **272,** 18460–18466
6. Schaeffer, M. L., Khoo, K. H., Besra, G. S., Chatterjee, D., Brennan, P. J., Belisle, J. T., and Inamine, J. M. (1999) *J. Biol. Chem.* **274,** 31625–31631
7. Kremer, L., Gurcha, S. S., Bifani, P., Hitchen, P. G., Baulard, A., Morris, H. R., Dell, A., Brennan, P. J., and Besra, G. S. (2002) *Biochem. J.* **363,** 437–447
8. Kordulakova, J., Gilleron, M., Mikusova, K., Puzo, G., Brennan, P. J., Gicquel, B., and Jackson, M. (2002) *J. Biol. Chem.* **277,** 31335–31344
9. Lee, Y. C., and Ballou, C. E. (1965) *Biochemistry* **4,** 1395–1404
10. Hill, D. L., and Ballou, C. E. (1966) *J. Biol. Chem.* **241,** 895–902
11. Apostolou, I., Takahama, Y., Belmant, C., Kawano, T., Huerre, M., Marchal, G., Cui, J., Taniguchi, M., Nakauchi, H., Fournie, J. J., Kourilsky, P., and Gachelin, G. (1999) *Proc. Natl. Acad. Sci. U. S. A.* **96,** 5141–5146
12. Cywes, C., Hoppe, H. C., Daffe, M., and Ehlers, M. R. (1997) *Infect. Immun.* **65,** 4258–4266
13. Hoppe, H. C., de Wet, B. J., Cywes, C., Daffe, M., and Ehlers, M. R. (1997) *Infect. Immun.* **65,** 3896–3905
14. Beatty, W. L., Rhoades, E. R., Ullrich, H. J., Chatterjee, D., Heuser, J. E., and Russell, D. G. (2000) *Traffic* **1,** 235–247
15. Jones, B. W., Means, T. K., Heldwein, K. A., Keen, M. A., Hill, P. J., Belisle, J. T., and Fenton, M. J. (2001) *J. Leukoc. Biol.* **69,** 1036–1044
16. Heldwein, K. A., and Fenton, M. J. (2002) *Microbes Infect.* **4,** 937–944
17. Takeda, K., Kaisho, T., and Akira, S. (2003) *Annu. Rev. Immunol.* **21,** 335–376
18. Sieling, P. A., Chatterjee, D., Porcelli, S. A., Prigozy, T. I., Mazzaccaro, R. J., Soriano, T., Bloom, B. R., Brenner, M. B., Kronenberg, M., Brennan, P. J., and Modlin, R. L. (1995) *Science* **269,** 227–230
19. Ernst, W. A., Maher, J., Cho, S., Niazi, K. R., Chatterjee, D., Moody, D. B., Besra, G. S., Watanabe, Y., Jensen, P. E., Porcelli, S. A., Kronenberg, M., and Modlin, R. L. (1998) *Immunity* **8,** 331–340
20. Severn, W. B., Furneaux, R. H., Falshaw, R., and Atkinson, P. H. (1998) *Carbohydr. Res.* **308,** 397–408
21. Vercellone, A., and Puzo, G. (1989) *J. Biol. Chem.* **264,** 7447–7454
22. Ludwiczak, P., Brando, T., Monsarrat, B., and Puzo, G. (2001) *Anal. Chem.* **73,** 2323–2330
23. Hoshino, K., Takeuchi, O., Kawai, T., Sanjo, H., Ogawa, T., Takeda, Y., Takeda, K., and Akira, S. (1999) *J. Immunol.* **162,** 3749–3752
24. Michelsen, K. S., Aicher, A., Mohaupt, M., Hartung, T., Dimmeler, S., Kirschning, C. J., and Schumann, R. R. (2001) *J. Biol. Chem.* **276,** 25680–25686
25. Takeuchi, O., Kawai, T., Muhlradt, P. F., Morr, M., Radolf, J. D., Zychlinsky, A., Takeda, K., and Akira, S. (2001) *Int. Immunol.* **13,** 933–940
26. Kawai, T., Adachi, O., Ogawa, T., Takeda, K., and Akira, S. (1999) *Immunity* **11,** 115–122
27. Muller, M., Eugster, H. P., Le Hir, M., Shakhov, A., Di Padova, F., Maurer, C., Quesniaux, V. F., and Ryffel, B. (1996) *Mol Med.* **2,** 247–255
28. Gilleron, M., Vercauteren, J., and Puzo, G. (1993) *J. Biol. Chem.* **268,** 3168–3179
29. Wang, Y., and Hollingsworth, R. I. (1995) *Anal. Biochem.* **225,** 242–251
30. Ozinsky, A., Underhill, D. M., Fontenot, J. D., Hajjar, A. M., Smith, K. D., Wilson, C. B., Schroeder, L., and Aderem, A. (2000) *Proc. Natl. Acad. Sci. U. S. A.* **97,** 13766–13771
31. Takeuchi, O., and Akira, S. (2002) *Curr. Top. Microbiol. Immunol.* **270,** 155–167
32. Goren, M. B. (1984) in *The Mycobacteria, a Sourcebook* (Kubica, G. P., and Wayne, L. G. eds) Vol. 15, Part A, pp. 379–415, Marcel Dekker, Inc., New York
33. Leopold, K., and Fischer, W. (1993) *Anal. Biochem.* **208,** 57–64
34. Nigou, J., Zelle-Rieser, C., Gilleron, M., Thurnher, M., and Puzo, G. (2001) *J. Immunol.* **166,** 7477–7485
35. Ballou, C. E., Vilkas, E., and Lederer, E. (1963) *J. Biol. Chem.* **238,** 69–76
36. Guerardel, Y., Maes, E., Elass, E., Leroy, Y., Timmerman, P., Besra, G. S., Locht, C., Strecker, G., and Kremer, L. (2002) *J. Biol. Chem.* **277,** 30635–30648
37. Lee, J. Y., Sohn, K. H., Rhee, S. H., and Hwang, D. (2001) *J. Biol. Chem.* **276,** 16683–16689
38. Netea, M. G., van Deuren, M., Kullberg, B. J., Cavaillon, J. M., and Van der Meer, J. W. (2002) *J. Immunol.* **23,** 135–139
39. Means, T. K., Wang, S., Lien, E., Yoshimura, A., Golenbock, D. T., and Fenton, M. J. (1999) *J. Immunol.* **163,** 3920–3927
40. Underhill, D. M., Ozinsky, A., Hajjar, A. M., Stevens, A., Wilson, C. B., Bassetti, M., and Aderem, A. (1999) *Nature* **401,** 811–815